



# Three combination value of extraction features on GLCM for detecting pothole and asphalt road

Yoke Kusuma Arbawa<sup>\*)</sup>, Fitri Utamingrum, Eko Setiawan

Faculty of Computer Science, Brawijaya University  
Veteran Road, Malang, Indonesia 65145

---

**Cara sitasi:** Y. K. Arbawa, F. Utamingrum, and E. Setiawan, "Three combination value of extraction features on GLCM for detecting pothole and asphalt road," *Jurnal Teknologi dan Sistem Komputer*, vol. 9, no. 1, pp. 64-69, 2021. doi: [10.14710/jtsiskom.2020.13828](https://doi.org/10.14710/jtsiskom.2020.13828), [Online].

---

**Abstract** – *The rate of vehicle accidents in various regions is still high accidents caused by many factors, such as driver negligence, vehicle damage, and road damage. However, transportation technology developed very rapidly, for example, a smart car. The smart car is land transportation that does not use humans as drivers but uses machines automatically. However, vehicle accidents are still possible because automatic machines do not have the intelligence like humans to see all the vehicle's obstacles. Obstacles can take many forms, one of them is road potholes. We propose a method for detecting road potholes using the Gray-Level Cooccurrence Matrix with three features and using the Support Vector Machine as a classification method. We analyze the combination of GLCM Contrast, Correlation, and Dissimilarity features. The results showed that the combination of Contrast and Dissimilarity features had the best accuracy of 92.033 %, with a computing time of 0.0704 seconds per frame.*

**Keywords** – *pothole; detection; GLCM; SVM; transportation*

## I. INTRODUCTION

Recently, researchers have studied autonomous technology, which is implemented in many ways, such as agriculture, space, and transportation. More interested researchers are in the field of transportation, mostly ground transportation. The intended ground transportation is an autonomous in-vehicle controller (unmanned ground vehicle), or what we know is a smart car [1].

Automated vehicle technology, such as smart cars, cannot be avoided by accidents. Vehicle accidents often occur due to many factors, such as negligence of the driver and the vehicle is not roadworthy due to road damage. Until 2017, there have been 103,228 accidents in all regions of Indonesia [2]. These accidents are caused by one of the factors above. Smart cars do not use humans to control vehicles. Therefore, it is possible for an accident if the smart car does not have good artificial intelligence.

Unmanned Ground Vehicles (UGV) can run on public roads using artificial intelligence planted on the vehicle. UGV is expected to be able to go through the streets by knowing what obstacles are in front of it. Several studies have examined the detection of obstacles on the road. However, they only focus on what vehicles and humans are in the front lane and road markings [3]. There is no research related to obstacles on the road, such as potholes. Pothole roads are dangerous for vehicles that can cause accidents due to shaking when passing a hollow road [4]. It is very dangerous if it happens to UGV, which does not have a crew as a decision supporter to avoid or reduce speed. The problem of detection of potholes can be overcome using computer vision technology (image/video).

Several studies have been conducted for pothole road detection. Hoang [5] studied pothole road detection using Steerable Filter-Based feature extraction with Least Square-Support Vector Machine classification. The results of this study found that the accuracy of perforated road detection was around 89%. The drawback of this study is that the author does not use texture analysis, so the results are not optimal.

Koch dan Brilakis [6] conducted another study; the detection of road holes on paved roads was carried out using a shape-based histogram to differentiate the perforated road from a normal road. However, the selection of road holes used for the dataset still uses the manual method. The accuracy results obtained in this study were 85% .

Wang et al. [7] conducted another study, pothole detection using GLCM, FCM, Wavelet, and classified with accuracy 86,7%. The drawback of the study is that no classification method was used. This paper only lists the level of accuracy, precision, and recall. This study also uses image data obtained from a google search, which is not real-time.

Sutrisno et al. [8] also researched potholes detection using the GLCM feature using the Neural Network as a classifier. This study results indicate that the proposed method successfully detects potholes with an accuracy of 86.6%. However, this study has shortcomings, and no evidence shows the computation time obtained in the test results. Therefore, it is not known how fast the Neural Network can identify potholes.

---

<sup>\*)</sup> Corresponding author (Yoke Kusuma Arbawa)  
Email: [yokekusumaarbawa@gmail.com](mailto:yokekusumaarbawa@gmail.com)

This study proposes the detection of potholes in real-time using the GLCM feature extraction, which is classified using Support Vector Machine (SVM). We use GLCM because the textures of the roads and potholes have different textures. It is important to analyze the texture features of GLCM to find out the best GLCM features to detect potholes. It also needs to calculate how fast the system is to detect potholes in real-time, as in the real situation. Three texture features have been obtained from GLCM, which are Contrast, Correlation, and Dissimilarity. We tested the combination of these three texture features, which was the most influential in detecting potholes. SVM has the advantage of accurate learning, hoping that the system could provide accurate and fast results.

## II. RESEARCH METHODS

### A. Dataset acquisition

The dataset was acquired at several road locations in Malang. The dataset has several different numbers and shapes of holes. Data was taken using a car dashboard camera with a size of 1280x720 pixels. The pothole detection process resizes the image to a size of 640x480 to speed up detection. The training data used are road drawings and 20x30 road hole images that Contrast, Correlation, and Dissimilarity features have extracted. Training data has two types, potholes and normal roads. In our research, positive data is potholes, and the negative data is the normal road, such as illustrated in Figure 1, respectively. This study used training data from manual cropping from pothole road images for each positive data and negative data. All data were extracted their features using GLCM. The total data training is 200 images: 100 images of positive data and 100 images of negative data. The testing data used were five videos with 24 frames per second with random pothole positions.

### B. Region of interest

Road detection requires the determination of the Region of Interest (RoI) of which part of the road will be detected as a pothole. In this study, the fixed RoI was used at the pixel index [250:280,200:500]. The RoI is the furthest position from the car that the hole in plain view can detect. The RoI used indicates the distance between the vehicle and the area to be detected. With this distance, the system is expected to provide an early warning to the vehicle. Figure 2 presents the RoI used in this research.

### C. Data processing

The detection of potholes uses per-frame images of car videos running on the road as the inputs. The road traveled by car has several holes. The image will be preprocessed first, resize the image and convert the color image to grayscale. The entire process is presented in Figure 3.

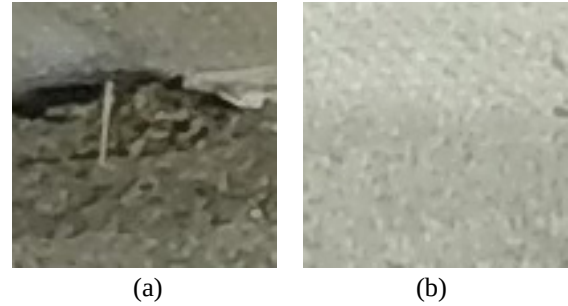


Figure 1. (a) Positive data (pothole road), (b) Negative data (normal road)

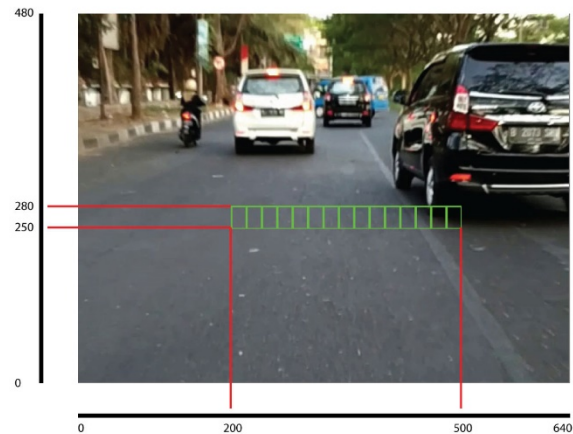


Figure 2. Illustration of RoI

The initial preprocessing is resizing the image to become 640x480. Image resizing is carry out to reduce the size of the image so that the classification process is done quickly. The GLCM process is carry out in a grayscale image. Images on each frame in RGB mode are converted to grayscale mode using (1). R denotes red color value of image in 8 bit, G green, and B blue color value. Each R, G, and B value has a different spectral power [9].

$$I_i = (0.299 \times R) + (0.587 \times G) + (0.114 \times B) \quad (1)$$

### D. GLCM feature extraction

This study used the GLCM feature extraction to get the value of the texture features from the image. GLCM extracts features in digital images using a statistical method of digital image pad features. This method can also be used to classify and distinguish different objects.

GLCM is a matrix of size  $n \times n$ ,  $n$  is the gray level value in the range of 0 to 255 for 8 bits of images [10]. GLCM considers the relationship between two pixels at a time, reference pixels, and offset pixels, as presented in Figure 4. The iteration of the algorithm through each reference pixel in-depth and comparing it to the offset pixel location offset determined by the angle of the reference pixel, as presented in Figure 5 [11].

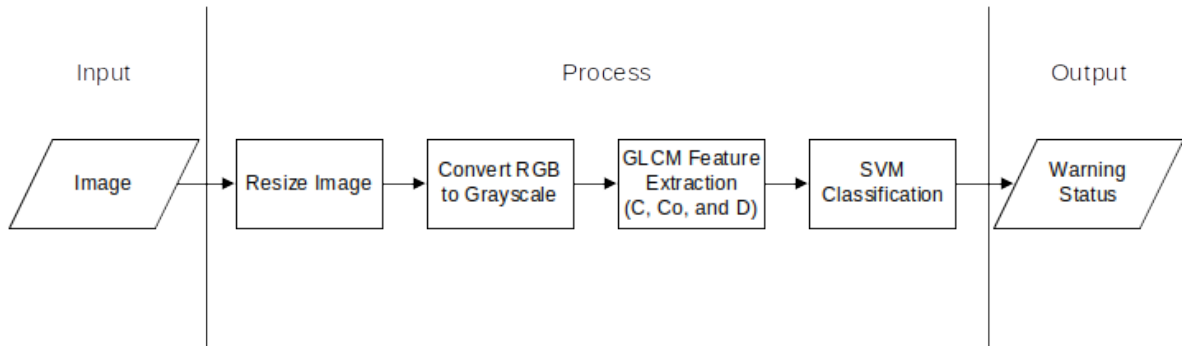


**Figure 3.** Proposed method

The path detection process accelerated by using only a few features of the GLCM. The proposed method uses contrast ( $C$ ), correlation ( $Co$ ), and dissimilarity ( $D$ ) texture features. The GLCM angle used is  $0$ , with the distance between the neighbors is  $1$ . Contrast ( $C$ ), correlation ( $Co$ ), and dissimilarity ( $D$ ) features calculation uses (2), (3), and (4) [12].

$$C = \sum_i \sum_j (i - j)^2 p(i, j, d, \theta) \quad (2)$$

$$D = \sum_i \sum_j p(i, j, d, \theta)^2 \quad (3)$$

$$Co = \left[ \sum_i \sum_j (ij) p(i, j, d, \theta) - \mu_x \mu_y \right] / \sigma_x \sigma_y;$$

$$\mu_x = \sum_i i \sum_j p(i, j, d, \theta) \quad \mu_y = \sum_j j \sum_i p(i, j, d, \theta) \quad (4)$$

$$\sigma_x = \sum_i (i - \mu_x)^2 \sum_j p(i, j, d, \theta)$$

$$\sigma_y = \sum_j (j - \mu_y)^2 \sum_i p(i, j, d, \theta)$$

### E. SVM classification

This study uses the SVM learning method based on the statistical learning theory [13]. The main purpose of SVM is to find the decision surface ( $H$ ) determined by certain points of the training data called the support vector between two class points [14]. The surface divides the training data ( $x_i, y_i$ ) without error. All points on the same class will be divided on the same side while the minimum distance between one of the two classes and the surface is the maximum margin value [15]. The surface present in Figure 6.

If the point is linearly separated, the function for this surface is determined by (5), with  $\alpha_i^*$  denotes Lagrange multiplier and  $b^*$  bias. If classes are not linearly separable, then the function for the surface is determined by (6), with  $k(x, y)$  is a kernel function.

$$f(x) = \text{sign} \left( \sum_{i=1}^n \alpha_i^* y_i (x_i, x) + b^* \right); (x_i, y_i) \in R^N \times [-1, 1] \quad (5)$$

$$f(x) = \text{sign} \left( \sum_{i=1}^n \alpha_i^* y_i k(x, y) + b^* \right) \quad (6)$$

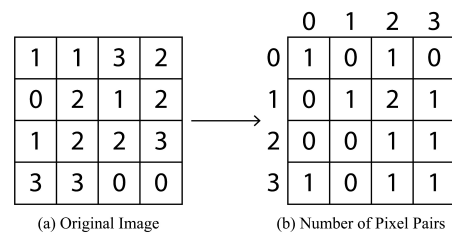


**Figure 4.** Determination of the GLCM matrix initial value

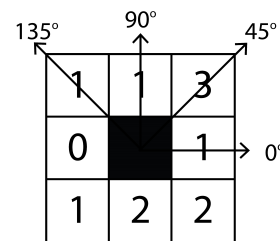


**Figure 5.** Common angles used in GLCM

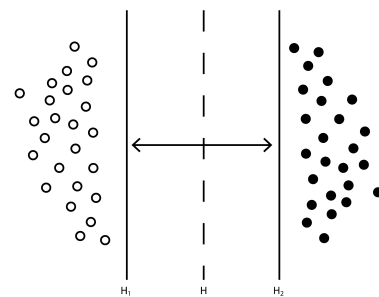


**Figure 6.** Optimal planes of SVM

This study uses the RBF kernel function to solve classes that are not linearly separable. The RBF kernel can provide high accuracy in the SVM classification. The RBF kernel formula uses (7), with  $x$  denotes  $i$  data,  $y$  is  $j$  data, and  $\sigma$  denotes standard deviation [16]. This study only use two classes that will be detected: pothole (positive data) and roads (negative data).

**Table 1.** Testing results using seven combination of features

Features	Accuracy (%)	Precision (%)	Recall (%)	Computation Time (sec)
C, Co, D	91.382	80.337	88.819	0.1206
C, Co	91.057	82.716	83.230	0.1256
C, D	92.033	83.333	86.957	0.0704
Co, D	89.268	76.243	85.714	0.0728
C	91.545	85.161	81.988	0.0630
Co	73.984	50.307	50.932	0.0740
D	91.707	82.738	86.335	0.0396

**Table 2.** Confusion matrix of testing data (C and D features)

Data	Total frame	TP	TN	FP	FN
V-01	1440	396	900	108	36
V-02	1440	324	1032	72	12
V-03	1440	324	1068	24	24
V-04	1440	360	936	84	60
V-05	1620	276	1176	48	120
	Accuracy			92.033 %	

\*TP = system detects potholes correctly, TN = system detects normal path correctly, FP = system detects normal roads as potholes, FN = system detects potholes as normal roads

$$k(x, y) = \exp\left(\frac{-|x-y|^2}{2\sigma^2}\right) \quad (7)$$

## F. Overall system and evaluation

The final result of this study is a warning system for a smart car. The warning system gives a red sign as a warning on roads that have holes. We also evaluate the accuracy and computational speed to determine our method's effectiveness providing a warning for potholes on the smart car. The algorithm performances are evaluated using (8) for accuracy, (9) for precision, and (10) for recall where *TP* denotes True Positive, *TN* as True Negative, *FP* as False Positive, and *FN* as False Negative.

$$Accuracy = \frac{TP+TN}{TP+FP+TN+FN} \quad (8)$$

$$Precision = \frac{TP}{TP+FP} \quad (9)$$

$$Recall = \frac{TP}{TP+FN} \quad (10)$$

## III. RESULTS AND DISCUSSION

This study used 100 positive data and 100 negative data as training data. The testing dataset is five videos with 24 frames per second with randomly positioned holes on the road. We conducted each test scenario for a combination of GLCM Contrast (*C*), Correlation (*Co*), and Dissimilarity (*D*) features. The combination obtained 7 combinations, namely (*C, Co, D*); (*C, Co*); (*C, D*); (*Co, D*); (*C*); (*Co*) and (*D*). Each combination uses the same processing method.

**Table 1** presents test results of all combinations. This results show that the best combination is only to use the Dissimilarity feature. Each feature shows different texture values and for different purposes. The Contrast shows the intensity level of sharpness (contrast) between the main pixel and its neighboring pixels. Correlation shows how similar pixels are between neighbors, whereas Dissimilarity shows the unequal distance between the main pixels and neighboring pixels.

From all combination features, the results obtained a small accuracy value of 73.984 % in testing using the Correlation feature. The other results also show the Dissimilarity value getting an accuracy value of 91.707%. The combination of Contrast and Dissimilarity features gains 92.033% accuracy. These results indicate that the combination of features compared to using only one feature gives equally good results. However, the best results are obtained when the system uses two combinations of features: texture features of Contrast and Dissimilarity. It gives better accuracy than [5]-[7]. The fastest computing time is 0.0396 sec when using the Dissimilarity feature only. These results are still not fast enough to be used in real-time warning systems.

**Figure 7** presents the testing data samples. Video data used for testing contains potholes that have random positions. From 1440-1620 frames tested on video 1 to video 5 (V-01, V-02, V-03, V-04, V-05), more data is a normal road than potholes. **Table 2** shows a confusion matrix table with two features C and D, getting the best accuracy value. The system can identify potholes well with 69-96 % correct. On video 1-4 the system has been detected well (only 276 correct out of 396 frames), but on video 5 the system cannot correctly detect any potholes. This incorrect detection is because the value of the GLCM feature (C and D) on the hollow road





**Figure 7.** (a) & (d) are frames that do not have potholes in the road, (b) & (e) are frames that have potholes in the road and (c) & (f) are ROI that has detected pothole in the road

frame is close to the normal road GLCM feature value. In testing using three features (C, D, and Co) in the fifth video, the system can better identify road holes with an accuracy value of about 75 % (300 of 396 frames). From these results, it can be concluded that if using the three features of the GLCM, the system can better identify potholes.

Combining the three proposed GLCM features provides a fairly good accuracy but not better than the one feature used (C) and (D). The test values for the computation time for the combination of three GLCM features show that the time is not fast enough compared to the combination of two features and one feature of GLCM. Compared with the research of Sutrisno et al. [8], SVM provides a better accuracy value than Neural Network. With this result, SVM can detect potholes well and provide fast enough time with the combination of two features or one GLCM feature.



**Figure 8.** System detects a road mark as a pothole

The detection of pothole road result is visualized in Figure 7. Pothole roads are marked in red, while roads that do not have holes are green. One example of incorrect detection is presented in Figure 8 which non-pothole detected as pothole, but it is actually a road mark. This incorrect detection is due to road markings have a texture similar to a pothole road.

The results of this study indicate a good accuracy and reasonably fast computation time. The use of the three GLCM features and classified using SVM is good for detecting potholes. This proposed method has the potential to be applied to UGV for the detection of potholes. In addition, this method can help further research in the field of digital image processing for detecting potholes roads.

#### IV. CONCLUSION

A new method of detecting potholes has been proposed using the GLCM features and SVM as a classifier. The proposed method can provide good accuracy and good computation time. The three GLCM features used in this study are suitable for the detection of potholes. In addition, SVM is excellent in identifying potholed roads compared to previous studies using neural networks. Further research could be carried out using other fast and precise classification methods related to the computational time needed in real-time.

#### REFERENCES

- [1] C. K. Y. Lam Loong Man, Y. Koonjul, and L. Nagowah, "A low cost autonomous unmanned ground vehicle," *Future Computing and Informatics Journal*, vol. 3, no. 2, pp. 304–320, 2018. doi: [10.1016/j.fcij.2018.10.001](https://doi.org/10.1016/j.fcij.2018.10.001)
- [2] Badan Pusat Statistik Indonesia, *Statistik transportasi darat 2017 (land transportation statistics 2017)*. Badan Pusat Statistik Indonesia, pp. 1–74, 2017.
- [3] Z. Zeng, T. Hu, and X. An, "Fast nonparametric road disparity estimation and gradient constrained obstacle detection for ugv navigation," *Journal of Physics: Conference Series*, vol. 1087, no. 6, 062010, 2018. doi: [10.1088/1742-6596/1087/6/062010](https://doi.org/10.1088/1742-6596/1087/6/062010)
- [4] H. Sawalakhe and R. Prakash, "Development of roads pothole detection system using image processing," *Intelligent Embedded System*, vol. 492, pp. 187–195, 2018. doi: [10.1007/978-981-10-8575-8\\_20](https://doi.org/10.1007/978-981-10-8575-8_20)
- [5] N.-D. Hoang, "An artificial intelligence method for asphalt pavement pothole detection using least squares support vector machine and neural network with steerable filter-based feature extraction," *Advanced in Civil Engineering*, vol. 2018, pp. 1–12, 2018. doi: [10.1155/2018/7419058](https://doi.org/10.1155/2018/7419058)
- [6] C. Koch and I. Brilakis, "Pothole detection in asphalt pavement images," *Advanced Engineering Informatics*, vol. 25, no. 3, pp. 507–515, 2011. doi: [10.1016/j.aei.2011.01.002](https://doi.org/10.1016/j.aei.2011.01.002)
- [7] P. Wang, Y. Hu, Y. Dai, and M. Tian, "Asphalt pavement pothole detection and segmentation based on wavelet energy field," *Mathematic Problems in Engineering*, vol. 2017, 1604130, pp. 1–13, 2017. doi: [10.1155/2017/1604130](https://doi.org/10.1155/2017/1604130)
- [8] I. Sutrisno et al., "Design of pothole detector using gray level co-occurrence matrix (glcm) and neural network (nn)," *IOP Conference Series: Materials Science and Engineering*, vol. 874, 012012, 2020. doi: [10.1088/1757-899X/874/1/012012](https://doi.org/10.1088/1757-899X/874/1/012012)
- [9] A. Güneş, H. Kalkan, and E. Durmuş, "Optimizing the color-to-grayscale conversion for image classification," *Signal, Image, and Video Processing*, vol. 10, no. 5, pp. 853–860, 2016. doi: [10.1007/s11760-015-0828-7](https://doi.org/10.1007/s11760-015-0828-7)
- [10] A. Chaddad, P. O. Zinn, and R. R. Colen, "Radiomics texture feature extraction for characterizing GBM phenotypes using GLCM," in *12th International Symposium on Biomedical Imaging*, Brooklyn, USA, Apr. 2015, pp. 84–87. doi: [10.1109/ISBI.2015.7163822](https://doi.org/10.1109/ISBI.2015.7163822)
- [11] F. Mohanty, S. Rup, B. Dash, B. Majhi, and M. N. S. Swamy, "Digital mammogram classification using 2D-BDWT and GLCM features with FOA-based feature selection approach," *Neural Computing and Applications*, vol. 32, pp. 7029–7043, 2019, doi: [10.1007/s00521-019-04186-w](https://doi.org/10.1007/s00521-019-04186-w)
- [12] M. A. Tahir, A. Bouridane, F. Kurugollu, and A. Amira, "Accelerating the computation of GLCM and haralick texture features on reconfigurable hardware," in *International Conference on Image Processing*, Singapore, Oct. 2004, pp. 2857–2860. doi: [10.1109/ICIP.2004.1421708](https://doi.org/10.1109/ICIP.2004.1421708)
- [13] P. C. Vasanth and K. R. Nataraj, "Facial expression recognition using SVM classifier," *Indonesian Journal of Electrical Engineering and Informatics*, vol. 3, no. 1, pp. 16–20, 2015. doi: [10.11591/ijeei.v3i1.126](https://doi.org/10.11591/ijeei.v3i1.126)
- [14] M. S. Tehrani, B. Pradhan, S. Mansor, and N. Ahmad, "Flood susceptibility assessment using GIS-based support vector machine model with different kernel types," *Catena*, vol. 125, pp. 91–101, 2015. doi: [10.1016/j.catena.2014.10.017](https://doi.org/10.1016/j.catena.2014.10.017)
- [15] S. Marianingsih and F. Utaminigrum, "Comparison of support vector machine classifier and Naïve Bayes classifier on road surface type classification," in *3rd International Conference Sustainable Information Engineering and Technology*, Malang, Indonesia, Nov. 2018, pp. 48–53. doi: [10.1109/SIET.2018.8693113](https://doi.org/10.1109/SIET.2018.8693113)
- [16] B. C. Kuo, H. H. Ho, C. H. Li, C. C. Hung, and J. S. Taur, "A kernel-based feature selection method for SVM with RBF kernel for hyperspectral image classification," *IEEE Journal of Selected Topics in Applied Earth Observations and Remote Sensing*, vol. 7, no. 1, pp. 317–326, 2014. doi: [10.1109/JSTARS.2013.2262926](https://doi.org/10.1109/JSTARS.2013.2262926)